

# Development of Diamond Tracking Detectors for High Luminosity Experiments at the LHC

## *The RD42 Collaboration*

M. Barbero<sup>1</sup>, V. Bellini<sup>2</sup>, V. Belyaev<sup>15</sup>, E. Berdermann<sup>8</sup>, P. Bergonzo<sup>14</sup>, H. Bol<sup>13</sup>, M. Bruzzi<sup>5</sup>, V. Cindro<sup>12</sup>, W. de Boer<sup>13</sup>, I. Dolenc<sup>12</sup>, P. Dong<sup>21</sup>, W. Dulinski<sup>10</sup>, V. Ermin<sup>9</sup>, R. Eusebi<sup>7</sup>, F. Fizzotti<sup>19</sup>, H. Fraiss-Kölbl<sup>4</sup>, A. Furgeri<sup>13</sup>, K.K. Gan<sup>17</sup>, A. Golubev<sup>11</sup>, A. Gorisek<sup>3</sup>, E. Griesmayer<sup>4</sup>, E. Grigoriev<sup>11</sup>, F. Hartjes<sup>16</sup>, H. Kagan<sup>17,◇</sup>, R. Kass<sup>17</sup>, G. Kramberger<sup>12</sup>, S. Kuleshov<sup>11</sup>, S. Lagomkarsino<sup>6</sup>, A. Lo Giudice<sup>19</sup>, I. Mandic<sup>12</sup>, C. Manfredotti<sup>19</sup>, A. Martemyanov<sup>11</sup>, M. Mathes<sup>1</sup>, D. Menichelli<sup>5</sup>, S. Miglio<sup>5</sup>, M. Mikuz<sup>12</sup>, M. Mishina<sup>7</sup>, S. Mueller<sup>13</sup>, H. Pernegger<sup>3</sup>, M. Pomorski<sup>8</sup>, R. Potenza<sup>2</sup>, S. Roe<sup>3</sup>, C. Schmidt<sup>8</sup>, S. Schnetzer<sup>18</sup>, T. Schreiner<sup>4</sup>, C. Schrupp<sup>21</sup>, S. Sciortino<sup>6</sup>, S. Smith<sup>17</sup>, R. Stone<sup>18</sup>, C. Suter<sup>2</sup>, M. Traeger<sup>8</sup>, W. Trischuk<sup>20</sup>, C. Tuve<sup>2</sup>, J. Velthuis<sup>1</sup>, E. Vittone<sup>19</sup>, R. Wallny<sup>21</sup>, P. Weilhammer<sup>3,◇</sup>, N. Wermes<sup>1</sup>

<sup>1</sup> Universität Bonn, Bonn, Germany

<sup>2</sup> INFN/University of Catania, Italy

<sup>3</sup> CERN, Geneva, Switzerland

<sup>4</sup> Fachhochschule für Wirtschaft und Technik, Wiener Neustadt, Austria

<sup>5</sup> INFN/University of Florence, Florence, Italy

<sup>6</sup> Department of Energetics/INFN Florence, Florence, Italy

<sup>7</sup> FNAL, Batavia, U.S.A.

<sup>8</sup> GSI, Darmstadt, Germany

<sup>9</sup> Ioffe Institute, St. Petersburg, Russia

<sup>10</sup> IPHC, Strasbourg, France

<sup>11</sup> ITEP, Moscow, Russia

<sup>12</sup> Josef Stefan Institute, Ljubljana, Slovenia

<sup>13</sup> Universität Karlsruhe, Karlsruhe, Germany

<sup>14</sup> LETI (CEA-Technologies Avancees) DEIN/SPE - CEA Saclay, Gif-Sur-Yvette, France

<sup>15</sup> MEPHI Institute, Moscow, Russia

<sup>16</sup> NIKHEF, Amsterdam, Netherlands

<sup>17</sup> The Ohio State University, Columbus, OH, U.S.A.

<sup>18</sup> Rutgers University, Piscataway, NJ, U.S.A.

<sup>19</sup> University of Torino, Italy

<sup>20</sup> University of Toronto, Toronto, ON, Canada

<sup>21</sup> UCLA, Los Angeles, CA, USA

◇ Spokespersons

## Abstract

During 2006 detectors based on new polycrystalline CVD (pCVD) material were produced as candidates for use in LHC experiments. The first full size diamond pixel module with ATLAS specifications using a  $2 \times 6 \text{ cm}^2$  pCVD sample was characterized in the 2006 CERN test beam. Radiation damage studies performed outside of CERN corroborate the radiation hardness of this material. Radiation hardness studies at CERN using the highest quality diamond were deferred until 2007 due to the PS magnet problem. ATLAS, CMS, ALICE and LHCb are planning to use diamond for their beam conditions monitoring systems. Construction of the BCM system for ATLAS was completed in 2006 and the BCM modules were characterized in 2006 CERN test beams. Similar devices are under construction for the CMS, ALICE and LHCb experiments. Single-crystal CVD (scCVD) samples were produced and made available to RD42 institutes. The first scCVD diamond pixel device was constructed and tested in the 2006 CERN test beams. In this report we present the progress and work done by the RD42 collaboration on the development of CVD diamond material for radiation detectors.

## 1 Introduction

With the commissioning of the LHC expected in 2007, progress in experimental particle physics in the coming decade will depend crucially upon the ability of experiments to take data in high radiation areas [1]. Already ATLAS and CMS are planning for detector replacements and high luminosity upgrades which require radiation hard technologies. Chemical Vapor Deposition (CVD) diamond has been used extensively in beam conditions monitors as the innermost detectors in the highest radiation areas of BaBar, Belle, CDF and all LHC experiments and has been discussed as an alternate sensor material for use very close to the interaction region of the LHC where extreme radiation conditions exist.

Over the past year the RD42 collaboration continued to work on CVD diamond detectors for high luminosity experiments at the LHC. The Collaboration has grown with the Ioffe Institute Moscow, ITEP Moscow, Josef Stefan Institute Ljubljana, MEPHI Institute Moscow and UCLA USA joining the effort. This R&D effort is growing as first attempts from the LHC community try to understand the radiation environment at the upgraded LHC, the Super-LHC(SLHC), and its consequences for detector design and implementation. In SLHC scenarios the total expected fluence at radii of about 5 cm will exceed  $10^{16}$  particles/cm<sup>2</sup>. Many studies are now being performed to find solutions for detectors which have to operate in these radiation environments. For silicon detectors material engineering, device engineering and change of detector operational conditions are envisaged. Other materials, 4H-SiC, GaN, CZT, *etc.* are also being examined. So far it is found that at such high fluences the operational conditions especially for silicon are extreme. The availability of a very radiation hard detector material and electronics will be of great importance in view of possible future luminosity upgrades for the LHC [1]. Thus there is considerable interest to continue investigations into CVD diamond material and optimization of CVD diamond for these radiation environments.

## 2 The RD42 2006 Research Program and Milestones

During the last year we have made great progress with diamond quality. Material with charge collection distance (ccd) of 300  $\mu$ m has been grown in wafer sizes with very good reproducibility. Transforming this technology to specific requirements of the LHC is ongoing. The first ATLAS diamond pixel module (which uses diamond from such a wafer) was constructed with the same bump-bonding and electronics that the present ATLAS silicon pixel modules use and tested in a high energy pion beam at CERN. The first irradiated single-chip ATLAS diamond pixel module was also tested in the pion beam at CERN. ATLAS has, during the last year, completed the construction of a Beam Conditioning Monitor (BCM) based on polycrystalline CVD (pCVD) diamonds. The first modules have been installed. The ALICE, CMS and LHCb experiments are also working on a BCM based on pCVD diamond material. Based on these successes an “Expression of Interest” for the ATLAS upgrade program based on pCVD diamond is being written. During the last year the first single-crystal CVD (scCVD) single-chip ATLAS diamond pixel module was tested. Material studies on scCVD material have continued as the delivered material grows in size.

### 2.1 The LHCC Milestones

The RD42 project was approved by the LHCC for continuation (CERN/LHCC 2006-020 LHC 81) with the following objectives:

- to construct and test diamond pixel detector modules with ATLAS/CMS front-end electronics,
- to pursue the development of single crystal CVD (scCVD) diamond material,
- to test the radiation hardness of the highest quality pCVD and scCVD diamond,
- to continue the development of systems for beam monitoring for the LHC and
- to strengthen the collaboration with future LHC applications.

## 2.2 Summary of Milestone Progress

New polycrystalline diamond material has recently become available, in the form of wafers, by our industrial partner, Element Six Ltd [2]. The collection distance of material from these wafers routinely exceeds  $300\ \mu\text{m}$ . Fig. 1 shows two such diamond wafers with as-grown collection distances of  $315\ \mu\text{m}$  and  $310\ \mu\text{m}$  respectively. During 2005 some difficulties were encountered in the processing the samples at Element Six. In some cases, a loss of charge collection was observed after the final processing depending on the details of the processing technique. Element Six has addressed this problem and it has not re-appeared.

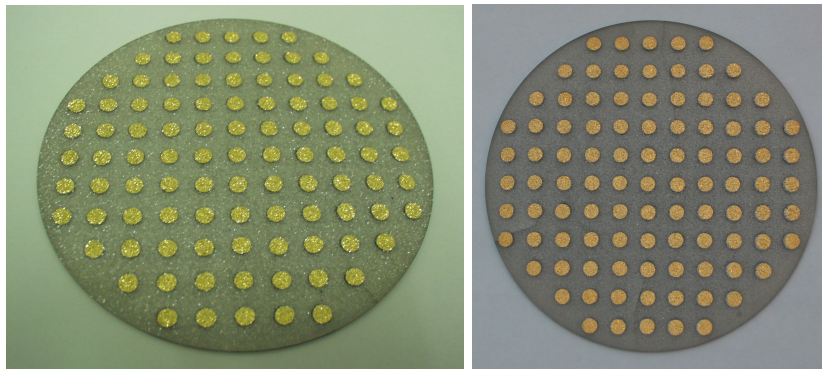


Figure 1: Photograph of the growth side of two full 12 cm wafers metalized with dots contacts 1cm apart for testing. The charge collected was measured at each dot on the wafer using a  $^{90}\text{Sr}$  source in the laboratory. The largest collection distances on these wafers is  $315\ \mu\text{m}$  and  $310\ \mu\text{m}$  respectively.

The production of high quality pCVD material has allowed RD42 to develop applications of diamond to high energy physics experiments. In collaboration with the groups developing front end electronics for both ATLAS and CMS, RD42 has constructed single-chip and multi-chip pixel modules. This past year we tested the first full diamond ATLAS pixel module ( $\sim 46,000$  channels) using diamond from one of the wafers shown above. This module used the final ATLAS IBM 0.25 micron rad-hard electronics and was bump-bonded and dressed in the same manner as all ATLAS pixel modules. The model was tested in the fall 2006 120 GeV pion test beam at CERN. This module performed quite well with a noise of  $136e$ , threshold of  $1450e$  and efficiency of  $>97\%$ . We also tested a single-chip pCVD ATLAS pixel module which has been irradiated to  $2 \times 10^{15}\ \text{p/cm}^2$ .

Three years ago RD42 began a research program to develop single-crystal CVD (scCVD) diamond. This type of diamond is grown in the same machines as pCVD material using a single-crystal substrate. Under these condition the CVD material copies the substrate producing a CVD material without grain boundaries. This past year both the thickness and size of the scCVD diamonds was increased. The thickest part produced with full charge

collection was  $880\ \mu\text{m}$ . The largest area part produced as part of a growth test was just over  $1.9\text{cm}^2$ . This past fall the first single-chip single-crystal ATLAS pixel module was constructed and tested in the 2006 CERN test beam. In addition, material studies on scCVD samples have been continued. On the first sample investigated with the TCT method we had found that this diamond had a positive space charge throughout the bulk, as reported in 2005. Many of the newer samples have been investigated in the same way and those samples did not exhibit any significant space charge. All samples again showed high low-field mobilities around  $2300\ \text{cm}^2/\text{Vs}$ , with holes always having higher mobilities than electrons. Charge collection showed saturation at electric field values above  $0.4\ \text{V}/\mu\text{m}$ . Carrier lifetimes in excess of the charge transit time through the whole thickness of the detector have been measured. This indicates that full charge collection is possible for detector thicknesses up to  $1\ \text{mm}$  operating at electric fields above  $0.5\ \text{V}/\mu\text{m}$ . Some interesting results from measurements with  $\alpha$  sources show very promising spectroscopy performance of scCVD samples.

As part of the radiation hardness program, RD42 irradiated the highest quality pCVD and scCVD diamond. We have reached a fluence of  $20 \times 10^{15}\ \text{p}/\text{cm}^2$  with pCVD diamond. After these fluences the diamonds were still working and characterized in test beams. We observed that after  $20 \times 10^{15}\ \text{p}/\text{cm}^2$  and operating at an electric field of  $1\text{V}/\mu\text{m}$  the diamonds still function well with 25% of the un-irradiated charge while at an electric field of  $2\text{V}/\mu\text{m}$  the diamonds have 33% of the un-irradiated charge. These studies will be repeated on additional samples and extended during the coming year as the CERN irradiation facilities become available.

RD42 together with BaBar, Belle, CDF, ATLAS, CMS, ALICE and LHCb are developing diamond detectors to provide radiation monitoring and abort protection for the various experiments. BaBar has taken the lead here and installed two pCVD samples in the IR between the beam-pipe and silicon vertex detector. Belle has installed two equivalent devices, CDF has installed thirteen pCVD devices and ATLAS has just completed the installation of eight stations with sixteen pCVD diamonds.

### 3 Progress on the Improvement of CVD Diamond Material

Over the last few years, we have worked closely with the Element Six [2] to achieve major improvements in the charge collection distance and uniformity of CVD diamond.

- pCVD diamond produced from production reactors now comes in  $12\ \text{cm}$  wafers.
- pCVD diamond produced from production reactors now regularly reaches  $300\ \mu\text{m}$  charge collection distance.
- scCVD diamond has been produced in production reactors in sizes larger than  $1\ \text{cm}^2$ .
- scCVD diamond produced from production reactors now regularly reaches full charge collection without any observable space charge.

The pCVD diamond research recipes have been migrated to production reactors. Production wafer diamonds are now planned for use in various experiments. The measured collection distance and pulse height distribution, using a  $^{90}\text{Sr}$  source, of a typical point on an as-grown wafer is shown in Fig. 2. To obtain this distribution we metalized the diamond with circular electrodes on each side. The mean charge is  $11,340e$  and the most probable charge is  $\approx 8000\ e$  and 99 % of the distribution is above  $4000\ e$ . From the mean value,  $\langle Q \rangle$ , of the signal spectrum one derives the charge collection distance

$$\bar{d} = \frac{\langle Q \rangle [e]}{36 e/\mu\text{m}} \quad (1)$$

where  $36 e/\mu\text{m}$  is the mean number of electron-hole pairs generated by a minimum ionizing particle along  $1 \mu\text{m}$  in diamond. The mean charge of  $11340 e$  corresponds to a charge collection distance of  $315 \mu\text{m}$ .

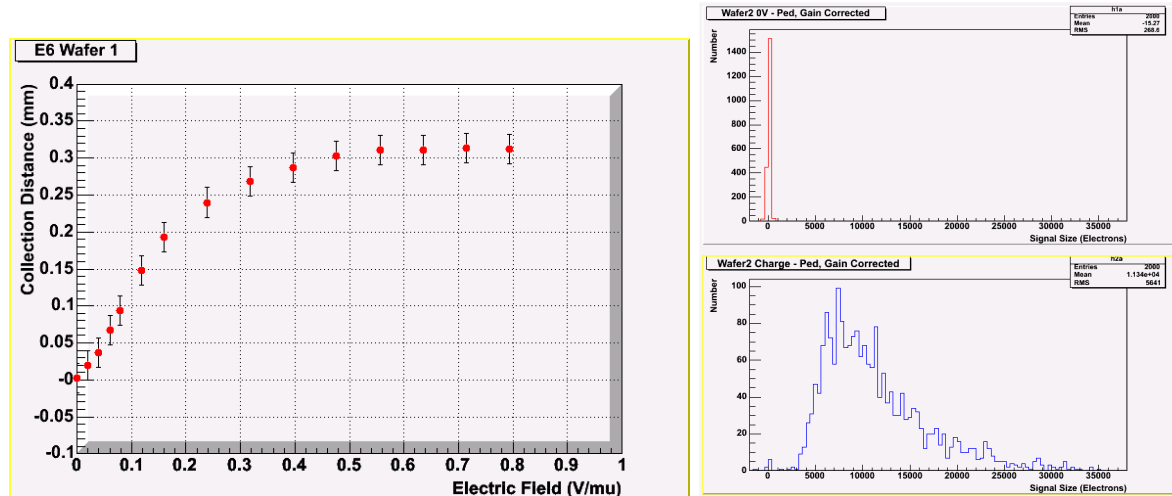


Figure 2: (a) Charge collection distance as a function of electric field and (b) Landau distribution measured with a  $^{90}\text{Sr}$  source in the laboratory. The histogram shown is taken using every scintillator trigger. The upper histogram is the observed pulse height with 0V applied to the diamond. The lower histogram is the observed pulse height at an electric field of  $0.7\text{V}/\mu\text{m}$ .

In the framework of the on-going research contract with Element Six to develop high electronic quality scCVD diamond samples with sizes exceeding  $1\text{cm}^2$  many more samples have become available in several RD42 institutes. Single-crystal CVD samples can be grown at present to sizes up to and exceeding  $1\text{cm}^2$ . Fig. 3 shows a photograph of four recently grown scCVD samples.

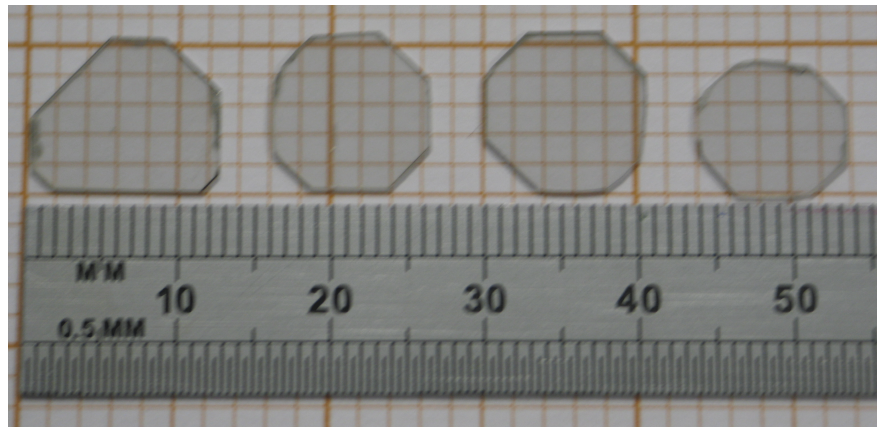


Figure 3: Photograph of four scCVD samples from the research contract.

In Fig. 4 we show the pulse height spectrum observed from four single crystal CVD diamonds. The diamonds are 210, 330, 435, and 685  $\mu\text{m}$  thick. We observe collection distances consistent with full charge collection; most probable charges of 5,500e, 9,500e, 13,400e and 21000e; FWHM's of 3000e, 3000e, 4000e, and 47000e; and more than 4,000e, 7,000e, 10,000e and 15,000e separation between the pedestal and the beginning of the charge distribution. The cutoff on the lower side of the Landau distribution occurs at about 75% of the charge at the Landau peak, which is more favorable than in silicon. The FWHM/MP for these single crystal CVD diamonds is approximately 0.3-0.5, about one third that of polycrystalline CVD diamond and about two thirds that of correspondingly thick silicon.

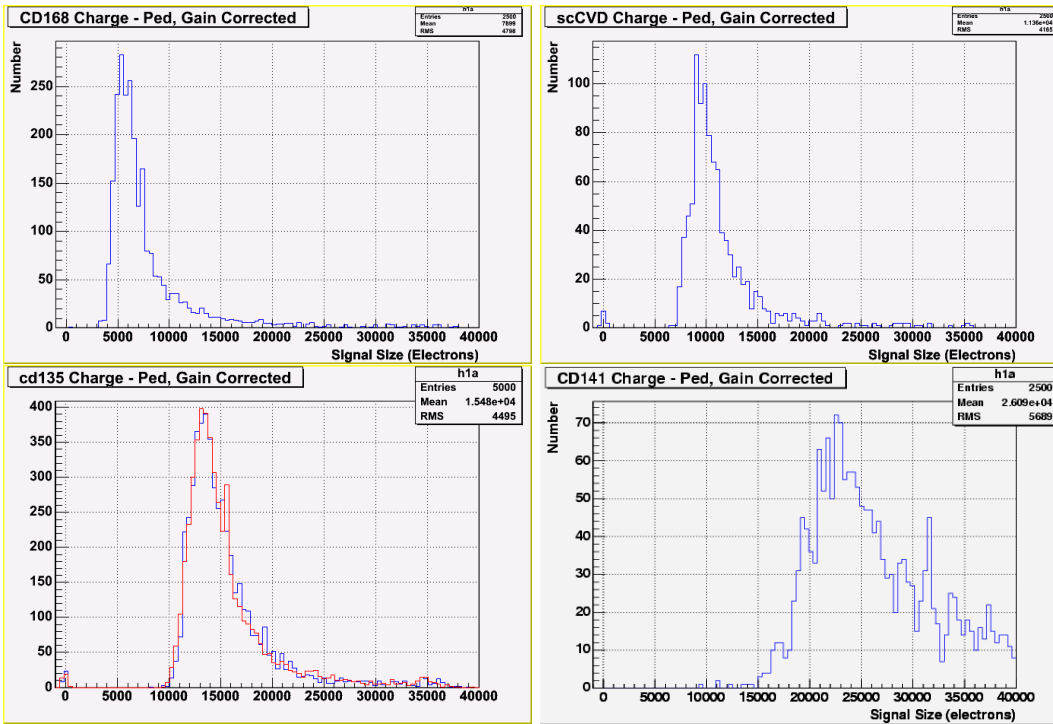


Figure 4: The pulse height distribution of various scCVD diamonds. The thicknesses of the diamonds are, from top left to to bottom right 210, 330, 435, 685  $\mu\text{m}$ . When there are two curves they are the results for positive and negative applied voltage.

In Fig. 5 we show the most probable charge for scCVD diamond versus thickness of the material. A clear linear relationship is evident out to thicknesses of 770  $\mu\text{m}$ . In order to understand the basic properties of this new material we began a program to measure the carrier lifetime and mobility by observing the transient current pulse when a particle penetrates a diamond and stops near the entrance electrode. The  $\alpha$  particles only penetrate about 14  $\mu\text{m}$  into the diamond bulk before they deposit all their energy. A fast current amplifier (rise time below 1 ns) is used to record the current pulses. Depending on the polarity of the electric field current pulses from holes or electrons are recorded separately, since the respective other charge carrier is instantly absorbed on the close electrode. The parameters we are able to extract from the data include transit time, velocity, lifetime, space charge independently for electrons and holes. Our first results [4] shown two years ago indicate that the carrier lifetimes in scCVD diamond are of the order of 35ns and that this particular diamond has a positive space charge in the bulk of the material. These measurements were repeated on several samples in 2006 obtained from Element Six. In Fig. 6 we show the current

pulses created by alpha particles injected on one surface of the scCVD diamond 480  $\mu\text{m}$  thick as a function of time. The newer material shows no evidence of space charge.

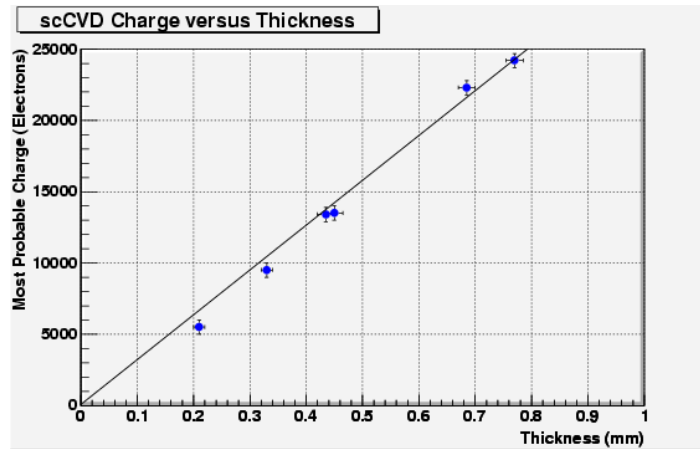


Figure 5: The most probable pulse height versus thickness for scCVD diamonds.

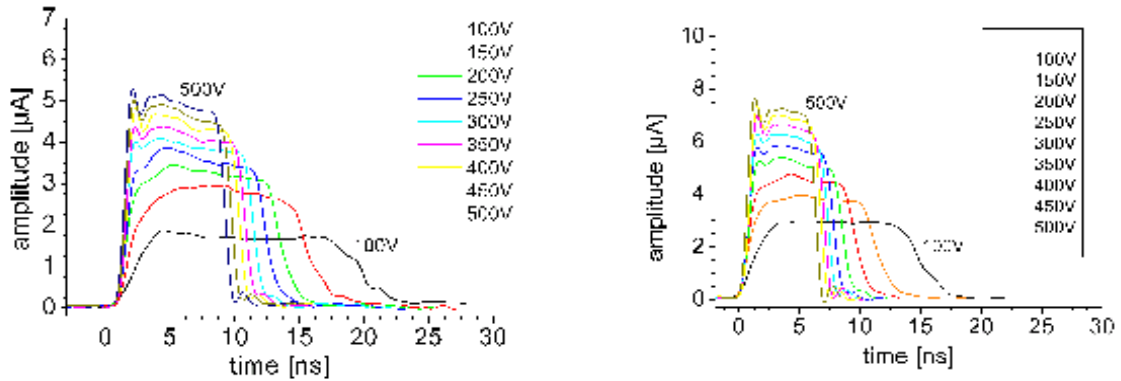


Figure 6: The observed current pulses created by alpha particles injected on one surface of the scCVD diamond as a function of time.

As indicated above the width of the Landau distribution is very narrow in scCVD diamond. This effect should translate into good energy resolution. In Fig. 7 we show the energy spectrum for  $\alpha$  particles from  $\text{Am}^{241}$ . An energy resolution of 17 keV FWHM is obtained indicating scCVD is spectroscopic grade material.

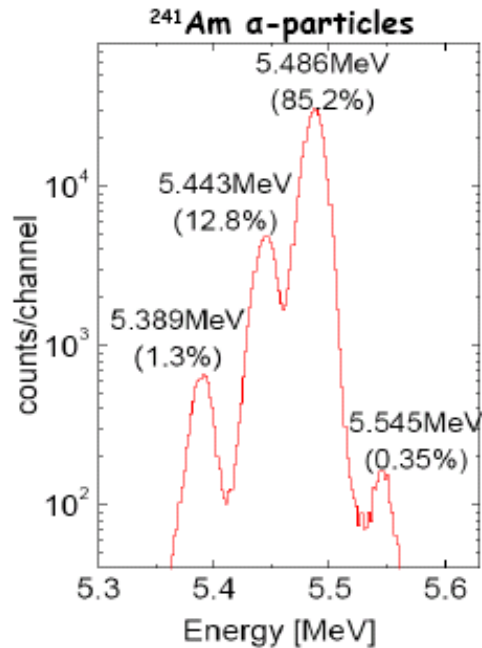


Figure 7: Energy spectrum obtained from an Am<sup>241</sup> α source with an scCVD diamond detectors. An energy resolution of 17 keV (FWHM) is observed.

## 4 ATLAS Pixel Modules

The production of high quality polycrystalline CVD material [2] with charge collection distance larger than 250 μm allowed RD42 to develop applications of diamond to high energy physics experiments. In collaboration with the groups developing front end electronics for ATLAS and the Fraunhofer Institute for Reliability and Microintegration (IZM) [5] for bump-bonding we constructed a range of diamond pixel detectors. Using the procedures developed for ATLAS, we constructed a full 2cm × 6cm diamond ATLAS pixel module, bump-bonded it to the final ATLAS IBM 0.25 μm rad-hard electronics, and tested the assembly at DESY and CERN. To date we have taken one million events in test beams at DESY in 2005 and 2006 and more recently 4 million events at CERN in 2006.

In Fig. 8 we show the final diamond pixel module with 16 pixel integrated circuit readout chips ready for external cables and testing. This module was tested at DESY in 2005 and at CERN in 2006 using the ATLAS telescope for external tracking.

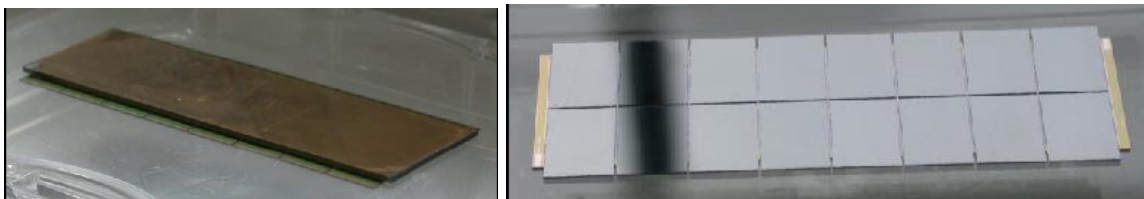


Figure 8: Photograph of the detector side (a) and electronics side (b) of the final ATLAS pixel module



Fig. 9 shows the module noise and threshold of the bare ATLAS pixel chip obtained in the laboratory. Fig. 10 and Fig. 11 show the tracking results obtained at DESY. Compared to a silicon module or 3D module the diamond module exhibits smaller noise ( $136e$ ), can be operated at lower threshold ( $1450e$ ) and attains a similar efficiency ( $>97\%$ ). The observed spatial resolution without correction is  $23\mu\text{m}$  in the  $y$ -view where the pixels have  $50\mu\text{m}$  pitch and a characteristic ‘top-hat’ distribution in  $x$  where the pixels are  $400$  and  $600\mu\text{m}$  long. In the low energy  $6\text{ GeV}$  beam at DESY the spatial resolution is dominated by multiple scattering. For example the silicon detectors in the telescope have an observed resolution of roughly  $7\mu\text{m}$  per plane at CERN and  $37\mu\text{m}$  per plane at DESY. It seems evident that this generation of diamond pixel detectors using the newly available larger collection distance diamond meet the specifications for applications at the LHC.

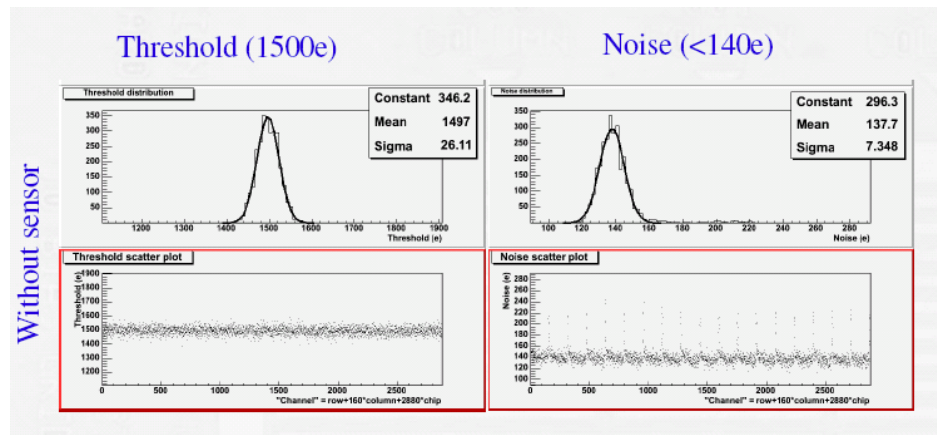


Figure 9: Bare (no detector) ATLAS pixel chip results for threshold and noise.

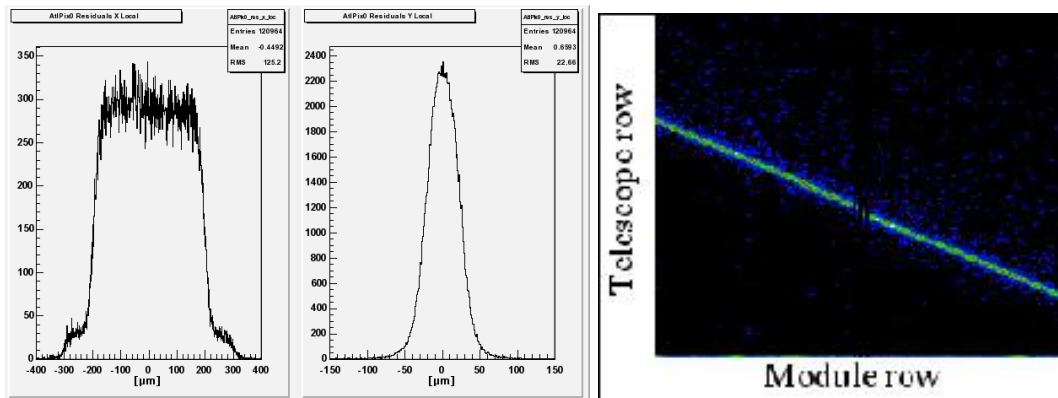


Figure 10: (a) Pixel module spatial resolution in the test-beam at DESY. The contribution from multiple scattering dominates the resolution and has not been unfolded. (b) ATLAS pixel module correlation with the tracking telescope.

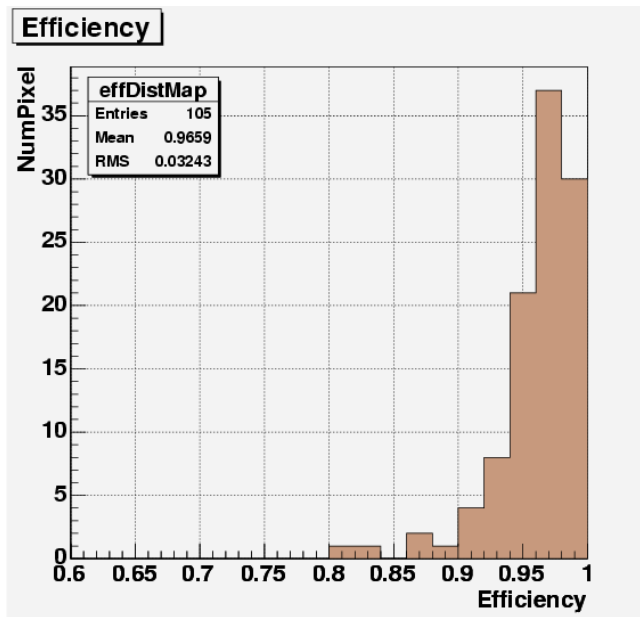


Figure 11: ATLAS pixel module preliminary efficiency.

This device was recently tested (Fall 2006) in the 120 GeV pion beam at CERN. Here as well the module noise was  $140e$  and the module operated at a threshold of  $1450e$ . Fig. 12 shows the raw online hit results for all scintillator triggers. Good correlation between the module and the telescope tracks is already observed at the raw trigger level. The analysis of this data is underway with final results expected in April 2007.

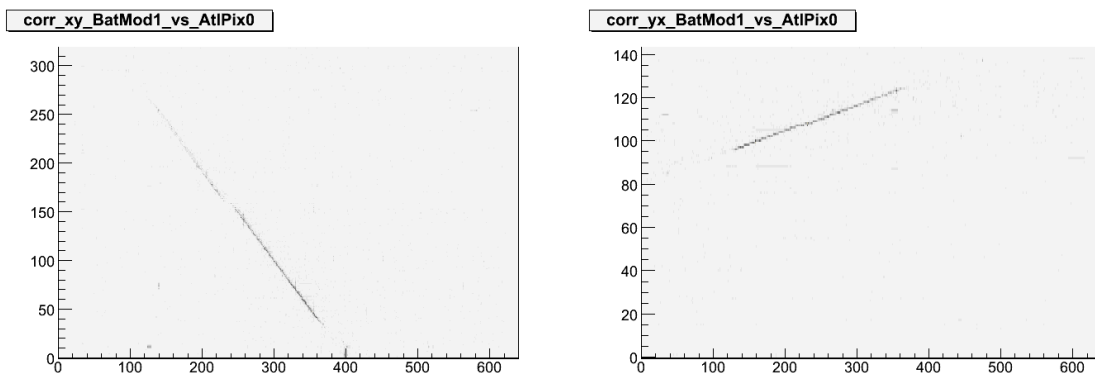


Figure 12: Correlation of the full ATLAS pixel module with the tracking telescope in  $x$  and  $y$  during the CERN 2007 beam test.

Recently we constructed a single-chip pixel module using one of the scCVD diamonds delivered from the research contract shown in Fig. 3. This single-chip scCVD diamond pixel module was bump-bonded at IZM in Berlin and uses the standard ATLAS pixel readout chip. The device was measured in the 120 GeV pion test-beam at CERN in Fall 2006. Fig. 13 shows the scCVD diamond before and after bump bonding. Fig. 14 shows the quality of the photolithography at the edge and center of the device. In Fig. 15 we show the 2D hit map of the single-chip scCVD pixel module. One observes the clear pattern of the beam and indicates the device is very efficient.

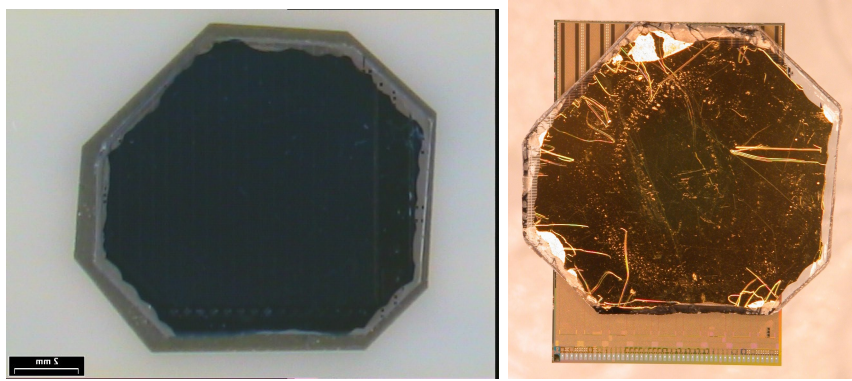


Figure 13: Photo of scCVD diamond pixel detector backside before (left) and after (right) bump bonding to the ATLAS pixel chip.

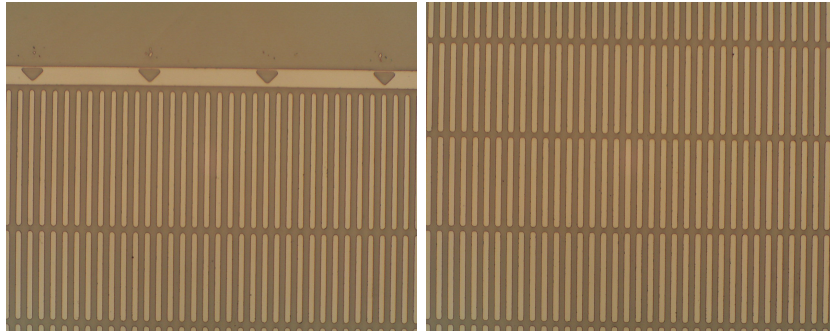


Figure 14: Photo of photolithography of the ATLAS pixel detector at one edge (left) and in the center of the detector (right).

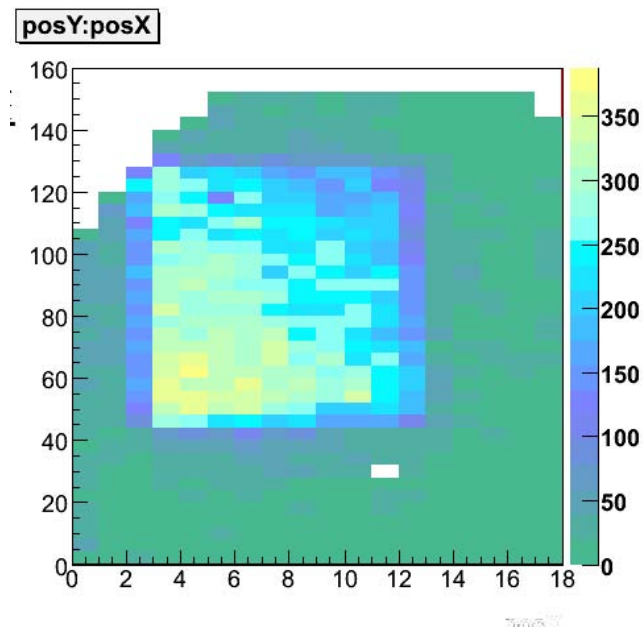


Figure 15: Hit map of the scCVD ATLAS pixel detector for events with a scintillator trigger and a track in the ATLAS telescope. The green area shows the outline of the detector. There is one dead pixel channel shown in white.

Fig. 16 shows the raw online data correlation for all triggers of the scCVD diamond pixel module with the nearest telescope plane in both coordinates. Even at the raw data level the correlation is quite evident.

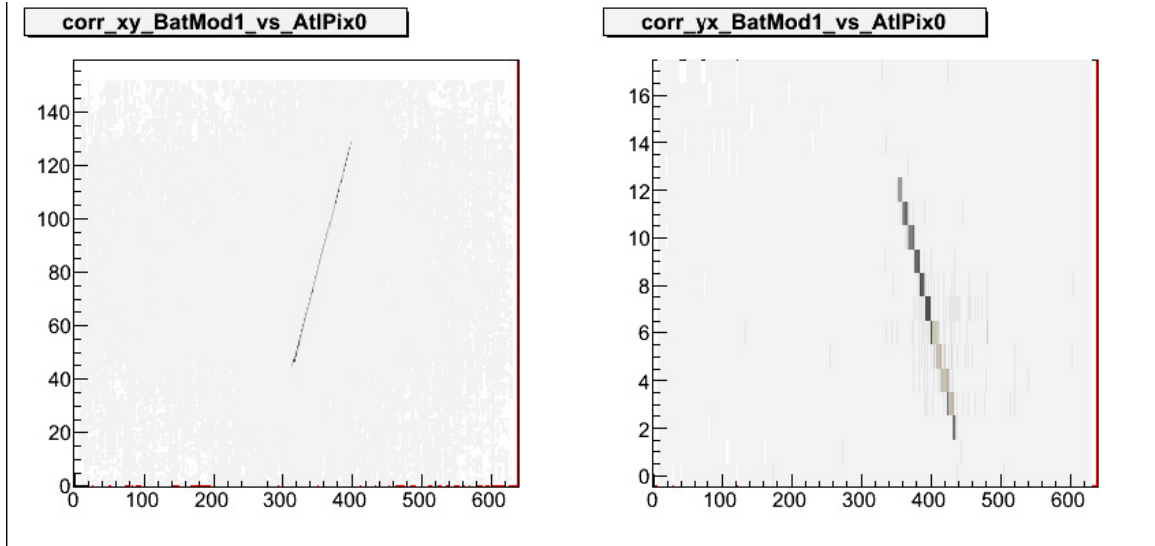


Figure 16: Online correlation of the hits in the scCVD diamond pixel detector with the Bonn telescope in both directions for all scintillator triggers.

Using the raw data we were able to compare the general characteristics of the scCVD diamond device at 100V and 400V. Fig. 17 and Fig. 18 show the Hits per Event and Pulse Height measured with a time over threshold (ToT) circuit at 100V and 400V. Using TOT the higher peak is the charge in single pixel hit events while the lower peak is the charge in multi-hit pixel events. The total charge observed from this device in single pixel hit events is roughly 14,000  $e$  and the device collects all the charge even at 100V ( $E=0.25 \text{ V}/\mu\text{m}$ ). We observe a trend toward more single pixel hits in both distributions as the voltage is raised.

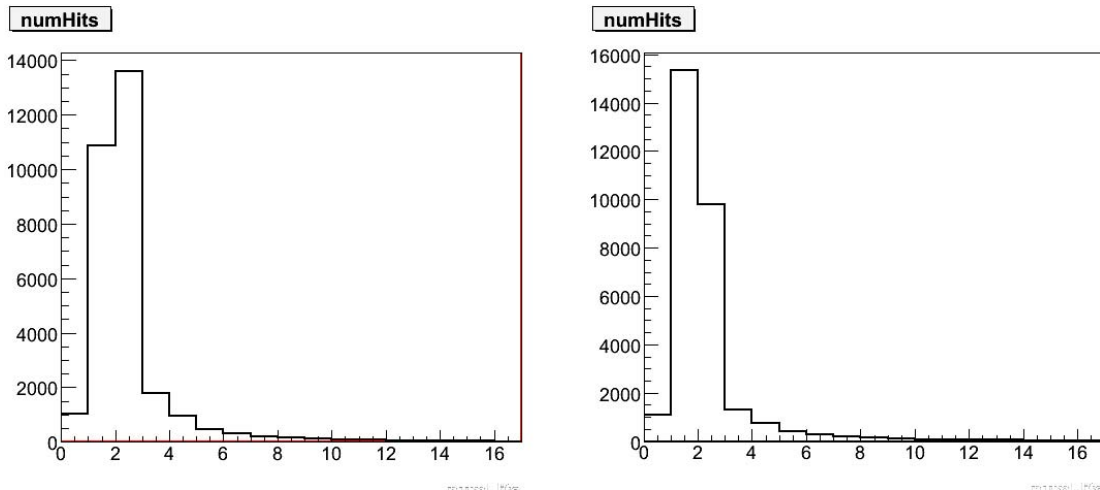


Figure 17: The number of Hits per Event Trigger at 100V operation (left) and 400V operation (right). As the voltage is raised we observe more single pixel hit events

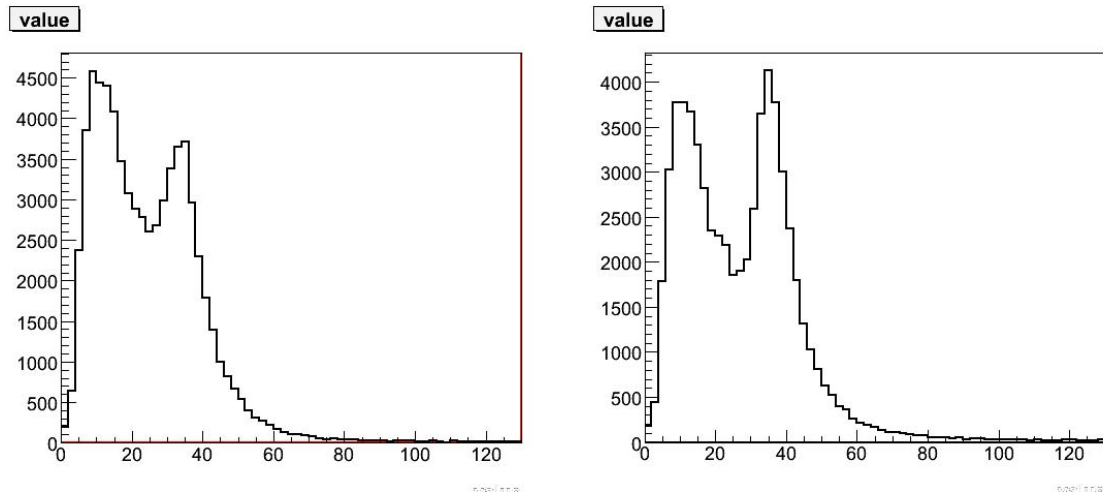


Figure 18: The Time Over Threshold (Pulse Height) at 100V operation (left) and 400V operation (right). The lower peak represents multi-pixel hit events; the upper peak is for single-pixel hit events. The rough calibration is 30 TOT is roughly 10,000 e. As the voltage is raised we observe more single pixel hit events

## 5 Radiation Hardness

In 2006 in order to obtain the most reliable irradiation results we chose to test each sample in the CERN test beam before irradiating the samples. Fig. 19 shows four scCVD samples prepared as strip detectors and read-out with VA-2 electronics for characterization in the test-beam at CERN. Fig. 20 shows the raw results of the pulse height for the first 36 events recorded by hand of one of the samples. A clear Landau is observed in the raw data with S/N larger than 100. Unfortunately when we had completed this beam test the irradiation facility at the CERN PS had problems. As a result none of these samples were irradiated in 2006. We now plan to complete this program in 2007.

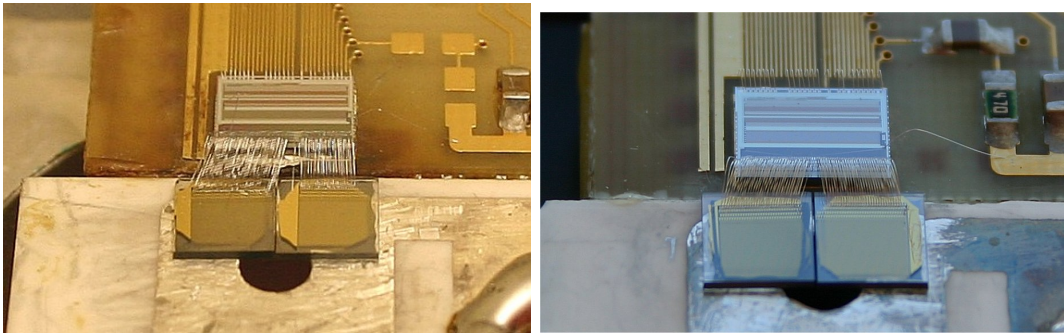


Figure 19: Photographs of the four scCVD samples characterized in the 120 GeV pion beam at CERN in Fall 2006.

In the remaining part of this section we present the summary of results on radiation hardness of diamond samples which was shown previously. In addition we present two new items: data on the effect of raising the electric field after irradiation indicating that raising the electric field yields more signal after  $18 \times 10^{15}$  p/cm<sup>2</sup> and a calculation and comparison with data of the NIEL hypothesis in diamond.

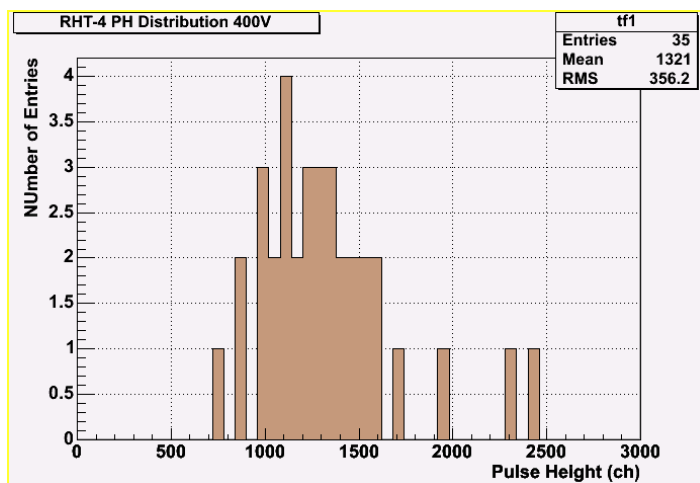


Figure 20: The raw pulse height from one of the scCVD strip detectors taken online during the test beam. A single pedestal was used for all channels. A clear landau is observed. The noise is roughly 10 counts on the scale shown.

The results from previous irradiations [7], [8], [9], repeated here for completeness, show that up to  $2.2 \times 10^{15}$  p/cm<sup>2</sup> pCVD diamonds lose at most 15% of the most probable charge and improve their resolution by roughly 40%. In Fig. 21, we show the previous results for the collected charge from a polycrystalline diamond strip detector after irradiation with a fluence of 24 GeV protons of  $1 \times 10^{15}$  p/cm<sup>2</sup> and after  $2.2 \times 10^{15}$  p/cm<sup>2</sup>. While the strip contacts before and after irradiation with fluences of  $1 \times 10^{15}$  p/cm<sup>2</sup> were unchanged the contacts were replaced after a fluence of  $2.2 \times 10^{15}$  p/cm<sup>2</sup> and then characterized in the test beam. This step was necessary since the wire bond pads were only usable twice. At  $1 \times 10^{15}$  p/cm<sup>2</sup> we observe that the shape of the signal-to-noise distribution is narrower than before irradiation and entries in the tail of the distribution appear closer to the most probable signal. At  $2.2 \times 10^{15}$  p/cm<sup>2</sup> and after re-metalization we observe essentially the same signal-to-noise distribution (measured with a low noise VA chip amplifier) as at  $1 \times 10^{15}$  p/cm<sup>2</sup> indicating that very little further damage occurred to the diamond bulk. The most probable signal-to-noise was 41 before irradiation and 35 at  $1 \times 10^{15}$  p/cm<sup>2</sup> and also at  $2.2 \times 10^{15}$  p/cm<sup>2</sup>. We find a reduction of maximum 15% in the most probable signal-to-noise after irradiation with  $2.2 \times 10^{15}$  p/cm<sup>2</sup>. The noise was measured to remain constant at each beam test. Since the beam test with the detector irradiated with a fluence of  $2.2 \times 10^{15}$  p/cm<sup>2</sup> used new contacts the observed decrease of 15% is attributed to damage in the diamond bulk.

Fig. 21 also shows residual distributions before irradiation, after  $1 \times 10^{15}$  p/cm<sup>2</sup> and after  $2.2 \times 10^{15}$  p/cm<sup>2</sup>. We observe that the spatial resolution improves from  $(11.5 \pm 0.3)$   $\mu$ m before irradiation to  $(9.1 \pm 0.3)$   $\mu$ m at  $1 \times 10^{15}$  p/cm<sup>2</sup> and to  $(7.4 \pm 0.2)$   $\mu$ m at  $2.2 \times 10^{15}$  p/cm<sup>2</sup>. At present the explanation for this effect is that the irradiated material is more uniform in the sense that the probability of large landau fluctuations has been reduced by the irradiation. The spatial resolution of nearly 7  $\mu$ m with a detector of 50  $\mu$ m strip pitch is comparable to results obtained with silicon detectors.

The RD42 group has now extended these irradiations to fluences up to  $18 \times 10^{15}$  p/cm<sup>2</sup> for pCVD material. This figure corresponds to a dose of roughly 500Mrad. 25% of its original pulse height.

In Fig. 22 we show a summary of the proton irradiation results described above. We find

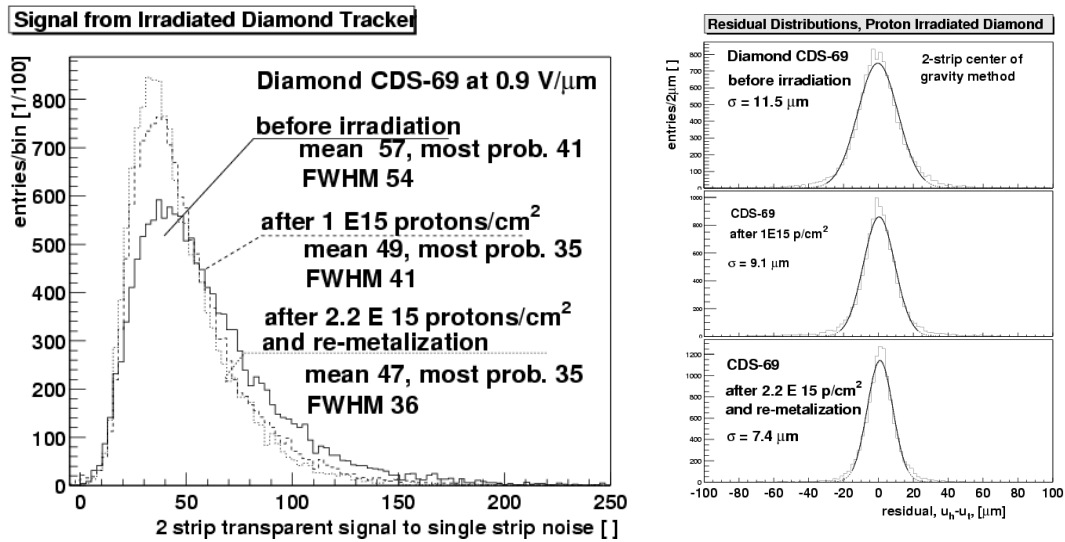


Figure 21: (a) Transparent 2-strip charge signal-to-noise distributions before (solid line), after proton irradiations with  $1 \times 10^{15}$  p/ $\text{cm}^2$  (dashed line) and after  $2.2 \times 10^{15}$  p/ $\text{cm}^2$  (dotted line). (b) Residual distributions before and after proton irradiation.

that all of the irradiations fall along an exponential curve. At an electric field of 1 V/ $\mu\text{m}$  we find the pCVD diamond retains 25% of its original charge and the diamond signal is down by 1/e at  $12.5 \times 10^{15}$  p/ $\text{cm}^2$ . Since the diamond signal is not saturated, one can collect more charge by raising the operating voltage. We observe at 2 V/ $\mu\text{m}$  the pCVD diamond retains 33% of the original charge.

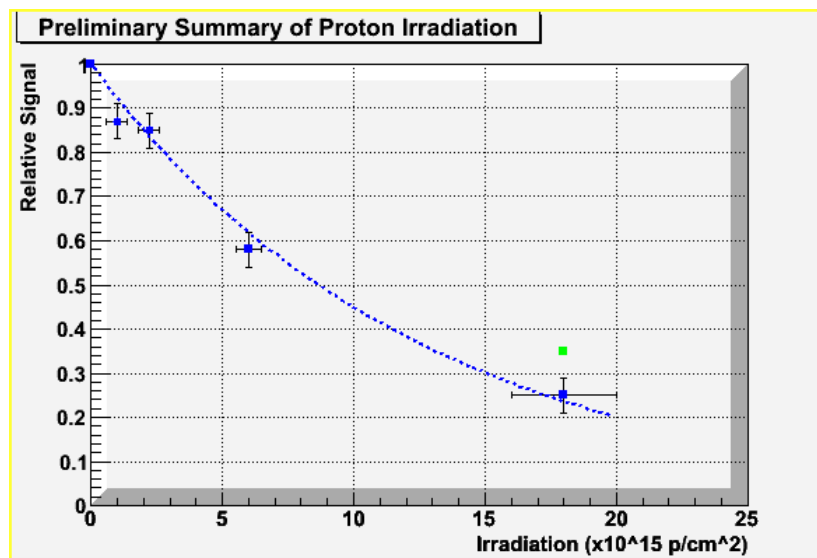


Figure 22: Summary of proton irradiation results for pCVD material at an electric field of 1 V/ $\mu\text{m}$  (solid circle points) and 2 V/ $\mu\text{m}$  (solid square point) to a fluence of  $18 \times 10^{15}$  p/ $\text{cm}^2$ . The blue curve is an exponential with exponent  $-0.08 \times \text{fluence}$  to guide the eye.

The Karlsruhe group of RD42 has performed a theoretical analysis to see if the NIEL hypothesis works for diamond material. The work used the package SRIM (Stopping and Range of Ions in Matter) for Coulomb scattering together with an add-on package to calculate nuclear interactions and fragment energy spectrum. The results of this study for the NIEL cross section for total, elastic and inelastic events are shown in Fig. 23 for both silicon and diamond. Also shown are the data points from three measurements in diamond at different energies for proton and neutron irradiation. The conclusion of this work is that at high energy radiation damage is dominated by the inelastic cross section while at low energy the radiation damage is dominated by the elastic cross section. Since silicon irradiation results fall on the silicon total cross section curve we conclude that in all cases we expect diamond to be more radiation hard than silicon.

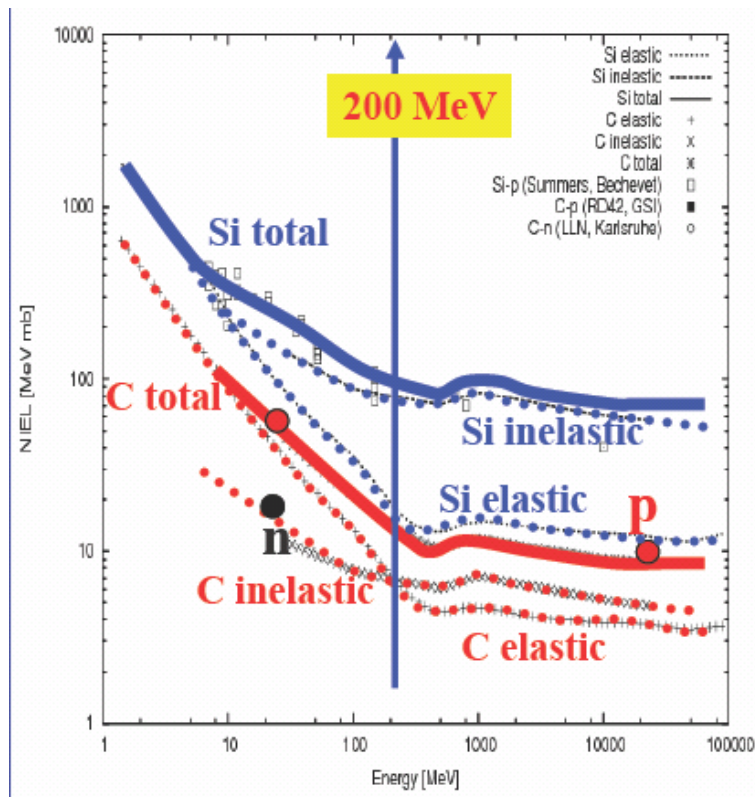


Figure 23: NIEL for total, elastic and inelastic events in silicon and diamond. Also shown are the data points from three measurements in diamond at different energies.

As indicated in Sec. 4 the diamond pixel module, due to its low capacitance and low leakage current operates at a lower noise level than a comparable silicon detector. We can compare the noise in one of the diamond pixel modules with that of a standard silicon pixel module or a 3D silicon pixel module all operating with the same electronics. We find the noise levels are  $140e$  for diamond,  $180e$  for silicon and  $310e$  for 3D silicon. In Fig. 24 we show the signal to noise as a function fluence for diamond pixels and 3D silicon pixels. The signal data for the diamond is taken from this report; the 3D silicon signal data is taken from the 3D silicon presentation at the Hiroshima Conference STD07 in Carmel.



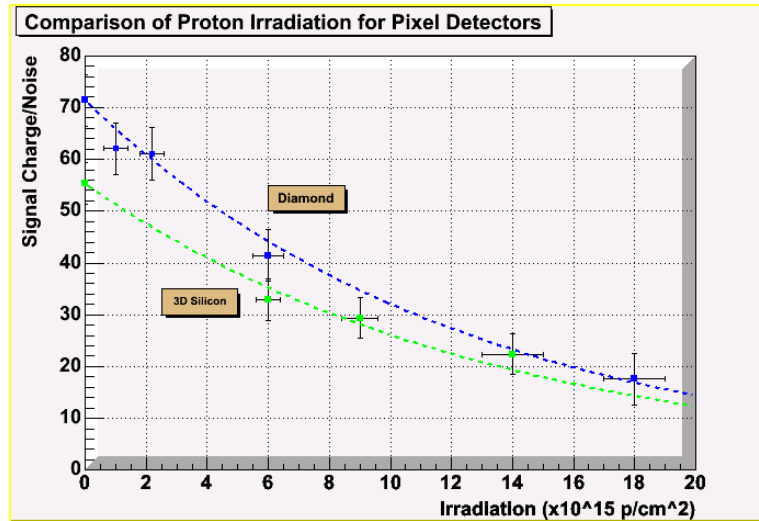


Figure 24: A comparison of Signal-to-Noise for irradiated diamond pixel modules and irradiated 3D silicon pixel modules using the same pixel electronics. The 3D silicon is operated at an electric field of roughly  $2\text{V}/\mu\text{m}$  while the diamond is operated at an electric field of  $1\text{V}/\mu\text{m}$ .

## 6 Beam Monitors

Radiation monitoring plays a crucial role in any experiment which operates a high precision tracking system close to the interaction region. Experience has shown that to protect the inner tracking devices systems must be provided which can abort the beams on large current spikes. In addition, radiation monitoring allows for the measurement of the daily dose and integrated dose which the tracking systems receive and thus allow the prediction of device lifetimes, etc.

Presently BaBar uses silicon PIN diodes for radiation monitoring inside of their silicon vertex detectors [13]. After  $100\text{fb}^{-1}$  the signal size for stable beams is approximately  $10\text{nA}$  while the leakage current in the PIN diodes is approximately  $2\mu\text{A}$ . Thus in these systems radiation monitoring is already becoming very difficult. Couple this with the fact that the PIN diodes must be temperature corrected continuously and one quickly finds that the radiation monitoring systems are a large effort to keep working. As a result BaBar has installed diamond replacements for the silicon PIN diodes. The main advantages of CVD diamond over silicon for this application is its small leakage currents, radiation hardness and temperature independent operation. Recently with the help of RD42 ATLAS and CDF have installed beam condition monitoring (BCM) systems based on pCVD diamond. We describe these below.

### 6.1 CDF Studies

The performance of a detector operating at hadron collider can be severely degraded by beam instabilities when high intensity, high energy particle beams are accidentally deflected into the detector and damage important detector components. To protect the detector from such accidents, fast, radiation hard beam condition monitoring detectors need to be installed which, if beam instabilities are detected, abort the beam safely and on the shortest time scale possible. Diamond detectors are ideal for this application. The largest system of this kind

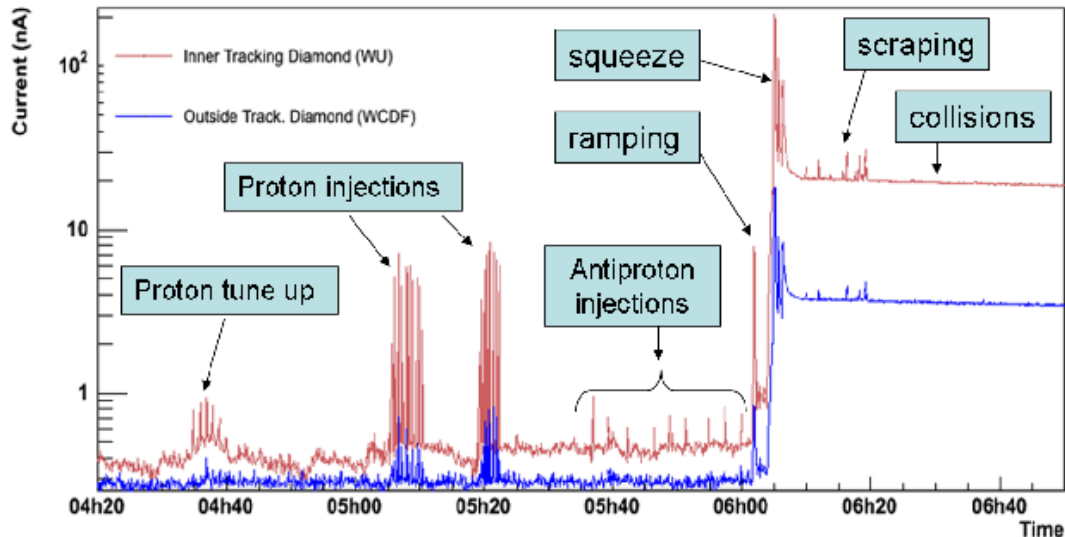


Figure 25: Diamond currents during beam injection at the Tevatron versus time. The current of one of the diamonds inside the tracking volume is shown (upper trace) together with the current outside the tracking volume, 20cm away from the beam (lower trace). The time granularity at which the data was accumulated is  $20 \mu\text{s}$ .

is currently operating at the CDF experiment at the Fermilab Tevatron. Overall 13 pCVD diamonds have been installed in the CDF detector. Eight diamond sensors have been installed inside the tracking volume. These sensors are immersed in a magnetic field of 1.4 T along the beam-line direction provided by the superconducting solenoid of CDF. These diamonds are divided in two groups of 4 located in the East and West side of the tracking volume. In addition, five more diamonds were installed in the outer side of CDF, where the baseline abort system, the Beam Loss Monitoring (BLM) system based on ionization chambers, is located. The diamonds are DC coupled and currents are readout over 80m of coaxial cable using custom built readout boards built by the Fermilab PPD electronics group [14] which affords a time resolution of up to  $20 \mu\text{s}$ . Data has been taken with this diamond BCM system during normal Tevatron operation. Figure 25 shows the response of two diamonds during the sequence of accelerator events leading to proton-antiproton collisions. One diamond is located 2.0cm from the beam inside the tracking volume while the other is located 20cm outside the tracking volume. This figure supports the clear advantage of the diamond closer to the beamline, as it can differentiate the structure of all the accelerator events, with respect to the diamond outside which cannot resolve these. While both these diamonds are biased and read out identically, the signal yield of the inner diamond is approximately an order magnitude larger than the outside one, representing the difference in radiation fields in both locations.

The abort functionality of this system is currently being commissioned by the CDF BCM group. In order to define suitable abort thresholds, beam incidents like the one recorded on November 9th, 2006 are used when a beam-abort signal was issued, due to a spark in the electrostatic capacitors separating the proton and anti-proton beams of the Tevatron accelerator. The data recorded in the buffers of the baseline BLM beam abort system and the novel diamond BCM system are compared. The data are shown in Figure 26. The

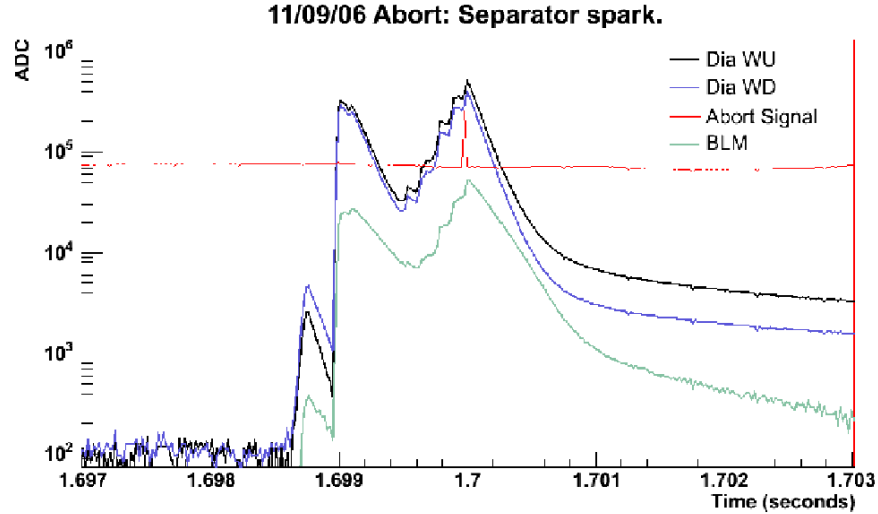


Figure 26: Time development of diamond and BLM currents in arbitrary ADC units versus time in seconds during the separator spark on 9th November 2006. The Figure shows the information for two diamonds (upper traces) and a BLM (lower trace). The flat line signals the moment of the arrival of the beam-abort signal at a relative time of about 1.7 seconds.

diamonds and the BLM report a three peak structure, but the diamond signals are an order of magnitude larger. The change in signal for the diamond spans three orders of magnitude, and first indications of beam instabilities are noticeable at least 1 millisecond (50 Tevatron revolutions) before the actual beam-abort signal was issued. Analysis of these types of beam instabilities are currently ongoing, and once a stable operating point is found, the beam abort functionality of the diamond BCM system will be enabled.

## 6.2 ATLAS Studies

ATLAS and CMS have a similar application to BaBar/Belle/CDF. The ATLAS experiment decided in 2005 to pursue a proposal to build a BCM detector based on pCVD diamond sensors. The aim is to detect minimum ionizing particles with good signal over noise ratio and a time resolution of  $\sim 1$  ns. The choice of diamond sensors was motivated by the radiation hardness of diamonds, the high charge carrier velocity leading to very fast and short current signal, very narrow pulses due to short charge carrier lifetime and very low leakage currents even after extreme irradiations. No detector cooling is needed.

In Fig. 27 we show a schematic view of the ATLAS BCM plan where the diamond monitors are placed in modules on the forward disks of the pixel detector. A module consists of a box housing two pCVD diamonds of  $1\text{cm} \times 1\text{cm}$  area with square contacts  $8\text{mm} \times 8\text{mm}$  mounted back to back. The signals from two sensors are fed in parallel into one channel of very high bandwidth current amplifiers. The design of a module is a S/N ratio of  $\sim 10:1$  in order to detect with high efficiency minimum ionizing particles.

Two stations will be installed symmetrically around the interaction region with 4 BCM modules mounted on each station. The stations will be installed at  $z = \pm 183.8$  cm (corresponding to 12.5 ns travel time of particles coming from the beam crossing) and  $r = 7$  cm and mounted on the pixel detector support structure. This structure will allow distinction between true bunch crossing interactions and beam interaction upstream and downstream of the interaction region in the beam pipe or in collimators by assigning very precisely a time

stamp to each signal. Signals with relative time stamps of 0ns, 25ns, 50 ns *etc.* come from the interaction region whereas signals with a time stamp difference in station one and station two come from other interactions due to beam instabilities. This system will monitor the stability of the proton beams on a bunch to bunch timescale. A very fast beam abort signal can be generated by this detector. In addition being positioned at a pseudo-rapidity of  $\sim 4$ , this detector can also be used to measure the instant luminosity in the LHC in addition to the ATLAS main luminosity detector LUCID.

The ATLAS system of consisting of 10 modules including spares has been constructed. Fig. 27 shows a finished module. In Fig. 28 we show the current signal observed for a single MIP (5 GeV/c pions) in an ATLAS BCM prototype module (a previous version of that shown in Fig. 27). The detector was read out through a 2-stage 500MHz current amplifier and a 16m long analog signal cable. The signal rises in under 1 ns and the average pulse width is 2.1ns.

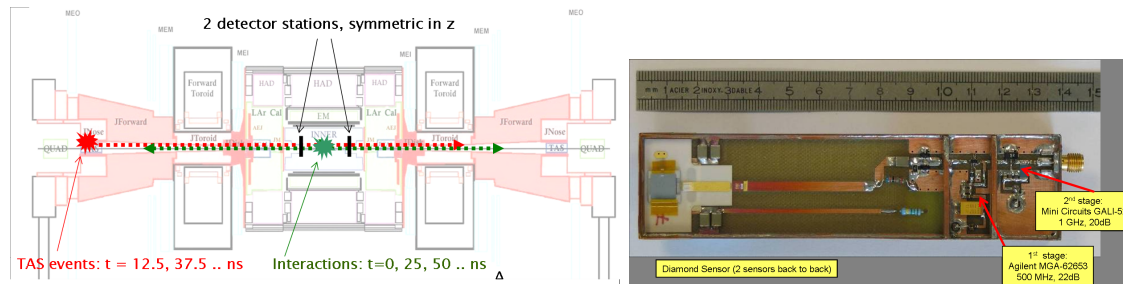


Figure 27: (a) A schematic view of the ATLAS BCM system. (b) A photograph of the final module used by ATLAS for its BCM system.

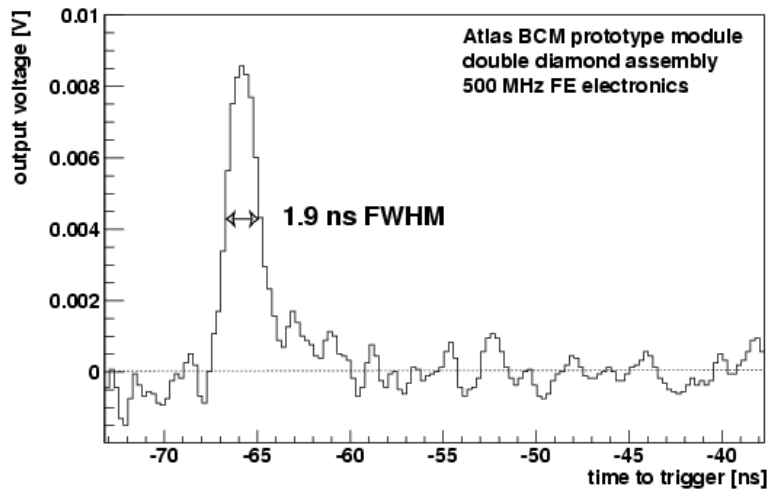


Figure 28: A scope trace of a MIP pulse observed in a BCM prototype double-decker diamond assembly in the ATLAS beam test.

In Fig. 29 we show the results for a final module in the Fall 2006 test-beam. The areas marked by a red box show the fiducial region with good track from the Bonn telescope used to determine the BCM parameters. For a module inclined at an angle of 45 degrees, the ATLAS BCM installation angle, we find a most probable signal of 280 and a noise of 20 indicating roughly a  $S/N=14:1$ .

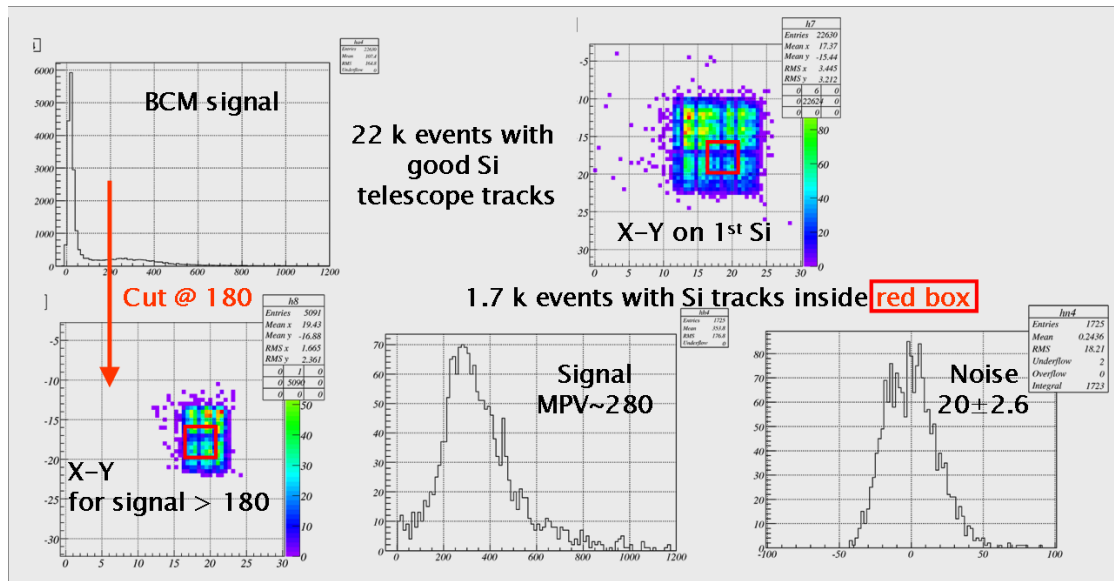


Figure 29: Results from the Fall 2006 beamtest with final modules. The fiducial region is marked in red and the signal and noise are shown.

The full BCM system has just been installed ATLAS. In Fig. 30 we show two photographs of the final installed ATLAS BCM in SR1.

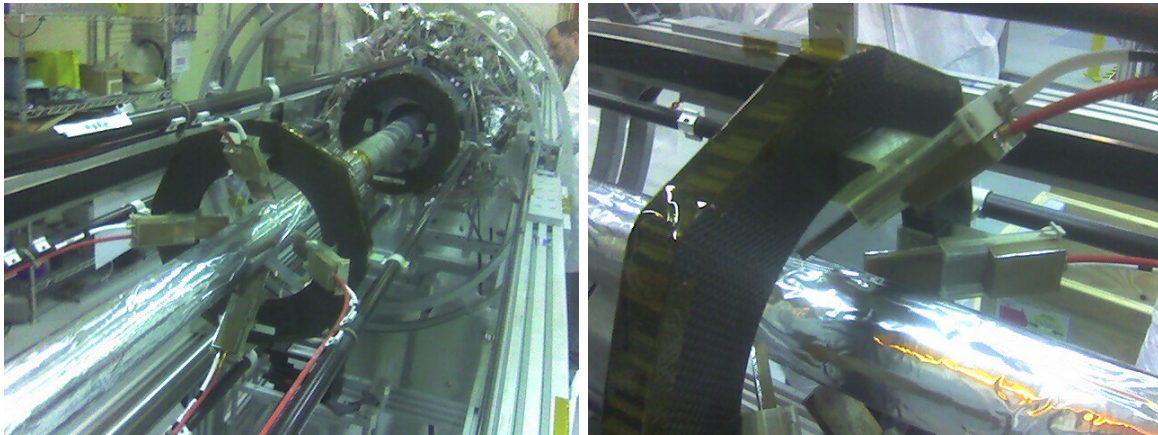


Figure 30: Photographs of the installed ATLAS BCM system in SR1. In the left image the ATLAS pixel detector is visible.

## 7 Proposed Research Program for 2007

The overall goal of the RD42 research program is to develop electronic grade CVD diamond and to demonstrate the usefulness and performance of CVD diamond as a radiation sensor material capable of detecting minimum ionizing particles in extremely high radiation environments. In order to achieve this goal the following main program steps had to be performed:

- Characterization of the electrical performance of specific CVD diamond samples grown

by Element Six and continuous feed back of results to the manufacturer.

- Irradiation of samples up to fluences of  $20 \times 10^{15}$  particles/cm<sup>2</sup>.
- Material science studies on these CVD diamond samples for defect characterization.
- Test of CVD diamond tracking devices with tailor made radiation hard front-end electronics for strip detectors and pixel detectors, including beam tests.

A large part of this program has been successfully achieved over the last years. There are however a number of important and decisive measurements still to be performed in this research program.

- A complete irradiation program for scCVD material and further irradiation studies with pCVD material have to be performed. Of particular importance are irradiations with protons up to and beyond  $10^{16}$  protons/cm<sup>2</sup> and with pions to the highest possible fluencies.
- Continued material characterization of pCVD and scCVD samples and extended material science studies including TCT measurements. Material science studies have been pursued in a number of RD42 institutes. This will be very important in producing reliably high quality CVD diamond radiation sensors.
- Beam tests with new tracking devices; double-sided strips and pixel modules.
- Collaboration on future applications like the ATLAS Pixel Upgrade proposition.

In summary, RD42 proposes to concentrate its efforts in 2007 in these areas.

- Pixel detectors, using the top quality CVD material available. This year we expect to transfer the technology for constructing a diamond module to industry. To this end construction of a second ATLAS pixel module is in progress. For this module the contacts will be produced in industry (IZM) as will reliable, efficient bump bonding. We propose to begin a third pixel module to gain statistical information on the process. We propose to test these modules in beam-tests at CERN with the latest radiation hard ATLAS and CMS front-end chips.
- Test of CVD diamond tracking devices with tailor made radiation hard front-end electronics for single-sided and double-sided strip detectors and pixel detectors in test beams.
- Characterization of the new, highest quality scCVD diamond material produced by Element Six under the research contract. Begin a systematic study of pCVD samples from as-grown to fully processed. Material science studies on these pCVD and scCVD diamond samples for defect characterization.
- Irradiation of pCVD and scCVD samples up to fluences of  $20 \times 10^{15}$  particles/cm<sup>2</sup> with protons, neutrons and pion beams using the highest quality diamond material. To this end we have prepared four scCVD diamond samples and characterized them in test beams at CERN in 2006. The proton irradiations are planned for 2007. In addition we propose to use four additional scCVD diamond characterise them in test beams at CERN before irradiation them in Ljubljana. Finally we propose to irradiate the first diamond ATLAS pixel module and characterize it in test beams at CERN.

## 8 Funding and Requests for 2007

As a result of the ongoing progress the RD42 project is supported by many national agencies and the total anticipated funding from sources outside CERN in 2007 is foreseen to be 150 kCHF. The majority of this funding is now through our North America colleagues who are funding the ongoing scCVD Research Program with Element Six. One reason why our collaborating institutes obtain national funding is that the RD42 project is officially recognized by CERN within the LHC R&D program. Official recognition of RD42 by CERN with the LHC R&D program has helped in the past to obtain funding from national agencies. For the continuation of the RD42 program as described in section 7 we request 50 kCHF of direct funds from CERN and that the LHCC officially approve the continuation of the program. This is essential to ensure future funding from national agencies. Furthermore a continuation of the RD42 program will be the basis of future diamond sensor development in the framework of R&D for future very high luminosity upgrades of the LHC, which is at present implemented [1]. It is foreseen that a minimal infra-structure for sample characterization and test preparation is maintained at CERN. The facility will be mainly used by external RD42 collaborators specifically ATLAS and CMS. We therefore request

- Maintain the present 20 m<sup>2</sup> of laboratory space in Bat.161 for test setups, detector preparation and electronics development.
- Maintain the present minimal office space for full time residents and visiting members of our collaboration.
- Three SPS test beam periods in 2007.
- Several irradiations in PS beam facility in 2007.

## References

- [1] 1st Workshop on Radiation Hard Semiconductor Devices for Very High Luminosity Colliders, CERN, 28-30 Nov. 2001.
- [2] Element Six Ltd., King's Ride Park, Ascot, Berkshire, SL5 8BP, United Kingdom.
- [3] Isberg, *et al.*, "High Carrier Mobility in Single-Crystal Plasma-Deposited Diamond", *Science* **297** (2002) 1670.
- [4] H. Pernegger *et al.*, "Charge-carrier Properties in Synthetic Single-crystal Diamond Measured with the Transient-current Technique", *J. Appl. Phys.* **97**, 073704 (Apr. 2005).
- [5] Fraunhofer Institut Zuverlässigkeit Mikointegration, Gustav-Meyer-Allee 25, D-13355, Berlin, Germany.
- [6] W. Adam *et al.* (RD42 Collaboration), "The First Bump-bonded Pixel Detectors on CVD Diamond", *Nucl. Instr. and Meth.* **A436** (1999) 326.
- [7] D. Meier *et al.* (RD42 Collaboration), "Proton Irradiation of CVD Diamond Detectors for High Luminosity Experiments at the LHC", *Nucl. Instr. and Meth.* **A426** (1999) 173.
- [8] W. Adam *et al.* (RD42 Collaboration), "Pulse Height Distribution and Radiation Tolerance of CVD Diamond Detectors", *Nucl. Instr. and Meth.* **A447** (2000) 244.
- [9] W. Adam *et al.* (RD42 Collaboration), "Performance of Irradiated CVD Diamond Micro-strip Sensors", *Nucl. Instr. and Meth.* **A476** (2002) 706.
- [10] W. Adam *et al.* (RD42 Collaboration), "A CVD Diamond Beam Telescope for Charged Particle Tracking" CERN-EP 2001-089.
- [11] W. Adam *et al.* (RD42 Collaboration), "Development of Diamond Tracking Detectors for High Luminosity Experiments at the LHC". Status Report/RD42, CERN/LHCC 2000-011, CERN/LHCC 2000-015.
- [12] W. Adam *et al.* (RD42 Collaboration), "Development of Diamond Tracking Detectors for High Luminosity Experiments at the LHC". Status Report/RD42, CERN/LHCC 2002-010, LHCC-RD-001.
- [13] A.J. Edwards *et al.*, "Radiation Monitoring with CVD Diamonds in BaBar" *Nucl. Inst. Meth.* **A552** (2005) 176.
- [14] R. Eusebi *et al.*, "A Diamond-based Beam Condition Monitor for the CDF Experiment", Proceedings of the 2006 IEEE Nuclear Science Symposium, to appear in *IEEE Trans. Nucl. Sci.*